Article

Deactivation of a Ce/TiO Catalyst by SO in the Selective Catalytic Reduction of NO by NH

Wenqing Xu, Hong He, and Yunbo Yu

J. Phys. Chem. C, **2009**, 113 (11), 4426-4432• DOI: 10.1021/jp8088148 • Publication Date (Web): 20 February 2009

Deactivation of a Ce/TiO_2 Catalyst by SO_2 in the Selective Catalytic Reduction of NO by NH_3

Wenqing Xu, Hong He,* and Yunbo Yu

Research Center for Eco-Environmental Sciences, Chinese Academy of Sciences, Beijing 100085, China

Received: October 6, 2008; Revised Manuscript Received: January 11, 2009

The effects of SO_2 on the selective catalytic reduction of NO by NH_3 over a Ce/TiO_2 catalyst were studied. Conversion of NO remained above 90% in the presence of 100 ppm SO_2 at 350 °C for 48 h. However, when 180 ppm SO_2 was added at 300 °C, NO conversion only remained above 90% during the first 12 h and then gradually decreased with time. Characterizations of fresh and SO_2-poisoned Ce/TiO_2 catalysts were carried out using Brunauer−Emmett−Teller method, ion chromatography, X-ray photoelectron spectroscopy, and X-ray diffraction. The analytical results indicate that there was no obvious change in the crystal structure of the different samples; however, the specific area decreased with SO_2 poisoning time. Sulfates were formed and preferentially diffused from the surface to a bulk phase during the poisoning process. Temperature-programmed desorption and diffuse reflectance infrared Fourier-transform spectroscopy results show that in the presence of O_2, SO_2 could react with NH_3 to form NH_4HSO_4, which is deposited on the surface of the catalyst and blocked the active sites. Moreover, the main reason for the deactivation is that SO_2 could react with the catalyst to form high thermally stable $Ce(SO_4)_2$ and $Ce_2(SO_4)_3$, resulting in the disruption of the redox properties between Ce(IV) and Ce(III) and the inhibition of the formation and adsorption of nitrate species.

Introduction

Nitrogen oxides (NO_x) emissions from both stationary and mobile fuel combustion sources pose serious environmental problems because of their contribution to acid rain, photochemical smog, ozone depletion, and greenhouse effects.[1] The selective catalytic reduction (SCR) of NO_x by NH_3 is a well-known technique used for the removal of NO_x from stationary power stations and diesel engines.[2−4] The $V_2O_5-WO_3/TiO_2$ and $V_2O_5-MoO_3/TiO_2$[5] catalysts have been widely applied in NO_x removal according to the following reaction: $4NO + 4NH_3 + O_2 \rightarrow 4N_2 + 6H_2O$. However, the toxicity of vanadium limits the development of these catalysts. Therefore, many researchers have recently focused on new catalysts, including zeolite and transition metal oxides. Among these, the zeolite catalysts, such as Fe-ZSM-5[6] and Fe-Ce-ZSM-5,[7] have been found to be highly active and selective for the reduction of NO by NH_3 over a broader temperature range and to be stable in the presence of SO_2 and H_2O. A large number of other transition metal oxide-based systems, such as MnO_x,[8] Cu/TiO_2,[9] and Fe_xTiO_y,[10] have also been extensively studied and thought to be promising alternatives to the V-based catalysts. We also recently reported a novel Ce/TiO_2 catalyst,[11] which was highly active in the SCR reaction within the temperature range of 275−400 °C and showed an excellent selectivity for N_2. Since typical coal and diesel fired exhausts contain variable amounts of SO_2, understanding the effects of SO_2 on SCR activity is important for the development and application of appropriate catalysts. The tolerance of metal oxide based catalysts to SO_2 depends on the type and oxidation state of the deposited metal, the nature of the support, and the kind of reducing agent. For example, chemical transformation of MnO to $MnSO_4$ was the main reason for the deactivation of the SCR over MnO_x.[12] In the case of V_2O_5/Al_2O_3,[13] the formation of aluminum sulfate during the SCR reaction in the presence of SO_2 reduced the surface area of the catalyst, which resulted in severe deactivation of the SCR catalyst. Ammonium bisulfate (NH_4HSO_4), which is a solid salt, also accumulated on the surface of V_2O_5/TiO_2 and interfered with the SCR reaction.[14] It has been determined that TiO_2 has an excellent sulfur tolerance because it is only partially and reversibly sulfated on its surface during the SCR reaction in the presence of SO_2.[15] Therefore, for the Ce/TiO_2 catalyst, we focused on the changes in the structure and state of the deposited metal oxides and the interaction between SO_2 and the reactants when the catalyst was exposed to SO_2 in a typical SCR reaction.

In the present study, we investigated the effects of SO_2 on the SCR of NO by NH_3 over the Ce/TiO_2 catalyst, characterizing the poisoned catalysts and the SO_2 poisoning mechanism. Brunauer−Emmett−Teller (BET), ion chromatography (IC), X-ray diffraction (XRD), X-ray photoelectron spectroscopy (XPS), and temperature-programmed desorption (TPD) methods were used to characterize the poisoned catalysts and to identify the surface and bulk sulfate species. A SO_2 deactivation process of Ce/TiO_2 in the SCR of NO by NH_3 is proposed using in situ diffuse reflectance infrared Fourier-transform spectroscopy (DRIFTS).

Experimental Section

Catalyst Preparation. The Ce/TiO_2 catalyst (Ce loading was 20.0 wt %) was prepared by an impregnation method using an anatase type TiO_2 (Shanghai Huijing Co. China) and an aqueous solution of cerium nitrate. The sample was dried at 110 °C for 12 h followed by calcination at 500 °C in air for 3 h. Finally, the catalyst was crushed and sieved to 20−40 mesh size.

Techniques of Characterization. The nitrogen adsorption−desorption isotherms were obtained at−196 °C over the whole range of relative pressures, using Quantasorb-18 automatic

* To whom correspondence should be addressed. Phone: +86-10-62849123. Fax: +86-10-62923563. E-mail: honghe@rcees.ac.cn.

10.1021/jp8088148 CCC: $40.75
Published on Web 02/20/2009

equipment (Quanta Chrome Instrument Co. USA). Specific areas were computed from these isotherms by applying the BET method.

The sulfate formed over the Ce/TiO_2 catalyst was converted into a water-soluble sulfate, and the quantitative analysis was performed using a Metrohm 861 Advanced Compact Ion Chromatograph (IC, Metrohm, Ltd., Switzerland). The corresponding sulfur contents from different samples were calculated from the concentration of SO_4^{2-} based on the stoichiometry.

A computerized Rigaku D/max-RB Diffractometer (Japan, Cu Kα radiation, 0.154056 nm) was used to obtain XRD patterns. Scans were taken over a range of 2θ angles from 10 to 90° at a speed of 4° min^{-1}.

The XPS measurement was carried out on an ESCALAB Mark II spectrometer (Vacuum Generators, UK) using Al Kα radiation ($h\nu = 1486.6$ eV). The binding energy was corrected using the contaminated carbon (284.6 eV).

The $SO_2 + O_2$ TPD experiments were carried out in a flow of He (30 cm^3 min^{-1}) over 350 mg of the catalyst. Prior to the TPD experiment, all catalysts were pretreated at 500 °C for 1 h in a flow of 20% O_2/He to yield a clean surface, followed by cooling to 300 °C. The samples were treated with 4000 ppm SO_2 + 5% O_2/He (30 cm^3 min^{-1}) at 300 °C for 1 h and then purged by He for 30 min to flush the excess SO_2. During each TPD experiment the sample was heated at a rate of 30 °C min^{-1} to the final temperature of 900 °C, and *m/z* values of 64 and 32 were monitored online by a mass spectrometer (Hiden HPR20, UK).

In situ DRIFTS was performed with a Nexus 670 (Thermo Nicolet, USA) Fourier-transform infrared (FT-IR) spectrometer equipped with an in situ diffuse reflection chamber and a high-sensitivity mercury−cadmium−telluride (MCT) detector. The sample was finely ground and placed in a ceramic crucible in the in situ chamber. Mass flow controllers and a sample temperature controller were used to simulate the reaction conditions, such as the mixture of gases, pressure, and sample temperature, which were the same as those in the catalytic activity tests. Prior to each experiment, the catalyst was heated in situ in a flow of 5% O_2/N_2 at 500 °C for 30 min and then cooled to 300 °C. A reference spectrum of the catalyst in a flow of 5% O_2/N_2 was taken as the background. All the spectra were collected at a resolution of 4 cm^{-1} with an accumulation of 100 scans.

Activity Test. The catalytic reaction was carried out in a fixed-bed quartz flow reactor at atmospheric pressure. The reactor was a 6-mm inside diameter quartz tube with a thermocouple placed on the outside wall of the reactor to control the temperature of the furnace. About 0.6 mL of catalyst (20−40 mesh) was used in all experiments. The reactor was heated by a temperature-controlled furnace. The feed gases consisting of 500 ppm NO, 500 ppm NH_3, 5 vol % O_2, and 100 or 180 ppm SO_2 in N_2 were adjusted by mass flow controllers and introduced into the reactor with a total flow rate of 500 cm^3 min^{-1}, yielding a gas hourly space velocity (GHSV) of 50000 h^{-1}. Analysis of the NO concentration was carried out using the online Nexus 670 FT-IR spectrometer equipped with a gas cell having a volume of 2 dm^3.

Results and Discussion

Effect of SO_2 on the Catalytic Activity of Ce/TiO_2. The effect of the addition of SO_2 on the SCR of NO by NH_3 over the Ce/TiO_2 catalyst was monitored as a function of time on stream at 300 or 350 °C. As shown in Figure 1, a steady-state NO conversion of 99.8% at 350 °C was obtained in the absence of SO_2. The addition of 100 ppm SO_2 to the feed resulted in a slight decrease in NO conversion to a certain value of 92.5% after 48 h. In contrast, a more obvious decrease in SCR activity occurred upon the addition of 100 ppm SO_2 at 300 °C. The NO conversion activity declined to 59.8% at 48 h, suggesting that the reaction temperature plays an important role in NO reduction in the presence of SO_2. Furthermore, NO conversion decreased to 34.5% in the following 48 h when 180 ppm SO_2 was fed at 300 °C. These results demonstrate that the presence of SO_2 considerably deactivates the SCR reaction over Ce/TiO_2.

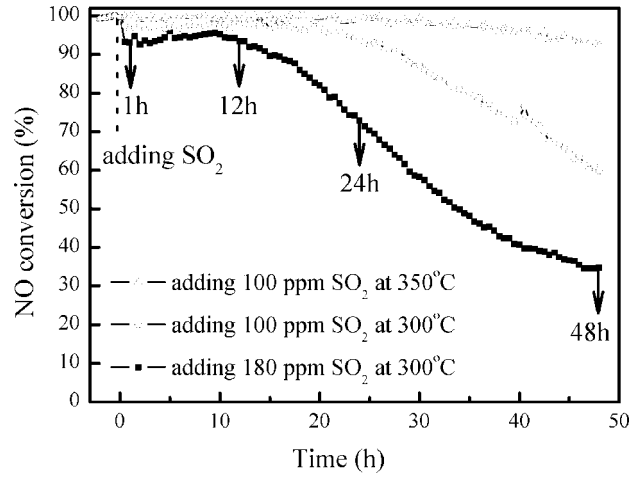

Figure 1. Effect of SO_2 on the SCR of NO with NH_3 over 20%Ce/TiO_2 catalyst.

TABLE 1: Specific Surface Areas and Sulfur Contents of Fresh and Poisoned Ce/TiO_2 Catalysts

sample (Ce/TiO_2)	BET surface area (m^2 g^{-1})	sulfur content (wt %)
S-0 h	128.6	-
S-1 h	124.5	3.00
S-12 h	97.7	6.12
S-24 h	90.8	8.05
S-48 h	82.5	11.76

To clarify the nature of the effects of SO_2 on the catalyst under different conditions, characterizations of the catalysts were performed. The poisoned catalysts under the reaction condition of 180 ppm SO_2 at 300 °C were chosen because the deactivation of Ce/TiO_2 by SO_2 was remarkable. Fresh and poisoned catalysts with different poisoning times are denoted as S-0 h, S-1 h, S-12 h, S-24 h, and S-48 h, respectively.

Reaction conditions were as follows: NO 500 ppm, NH_3 500 ppm, O_2 5%, SO_2 100 or 180 ppm, balance N_2, GHSV = 50000 h^{-1}, total flow rate 500 cm^3 min^{-1}, temperature 300 or 350 °C

Characterization of Poisoned Catalysts. The specific surface areas and sulfur contents of the fresh and poisoned Ce/TiO_2 catalysts are summarized in Table 1. Significant decreases in surface area were observed with increased time after the fresh Ce/TiO_2 catalysts were poisoned by SO_2. In addition, the sulfur contents of poisoned catalysts determined by IC also increased with poisoning time. It has been demonstrated that when sulfate species are formed and deposited on the catalyst the specific surface area of the catalyst decreases. Our results are consistent with studies[13] that showed that the decreasing surface area of a catalyst is one reason for the decrease in catalytic activity in the presence of SO_2.

The X-ray powder diffraction patterns of the fresh and poisoned Ce/TiO_2 catalysts are shown in Figure 2. All reflections showed typical diffraction patterns for the TiO_2 anatase phase

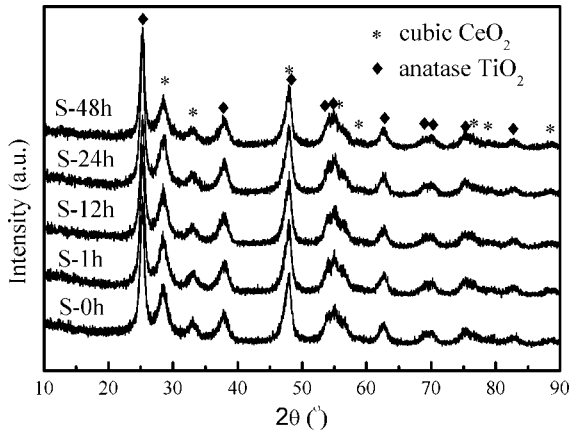

Figure 2. XRD patterns of fresh and poisoned Ce/TiO_2 catalysts.

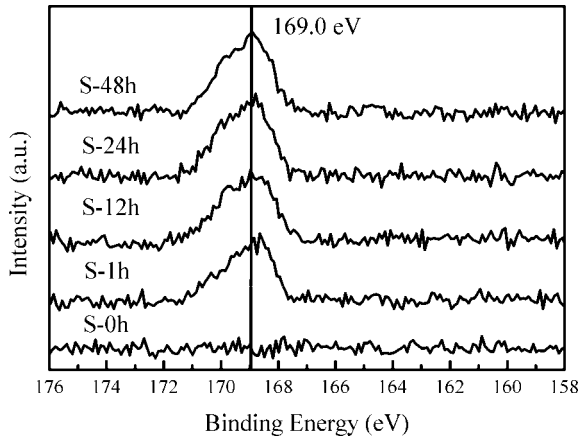

Figure 3. Experimental S2p XPS spectra of fresh and poisoned Ce/TiO_2 catalysts.

(PDF-ICDD 21-1272) and the cubic CeO_2 structure (PDF-ICDD 34-0394). With an increase in poisoning time, no obvious change was observed in the crystal structures of the different samples. Although more than 11% sulfur content was detected on the Ce/TiO_2 catalyst poisoned by 180 ppm SO_2 at 300 °C for 48 h, no new peaks ascribed to sulfate were observed, which suggests that either surface sulfate or an amorphous bulk sulfate formed on the surface of the catalyst.[12]

The catalysts were further analyzed using XPS to identify the surface nature and concentration of the active species. The representative photoelectron peaks of S2p and Ce3d pertaining to fresh and poisoned samples are depicted in Figures 3 and 4. The corresponding binding energies of $Ce3d_{5/2}$ and $S2p_{3/2}$, together with the Ce(III)/Ce ratio and sulfur weight percentages on the surface determined by XPS, are summarized in Table 2.

An essential difference in the sulfation of Ce/TiO_2 was exhibited in the behavior of the S2p and Ce3d lines. That is, the exposure of the fresh catalyst to SO_2 resulted in an appearance of an S2p feature (Figure 3). The $S2p_{3/2}$ binding energies, which are usually applied to elucidate the chemical state of sulfur,[16] are shown in Table 2. These data demonstrate that the $S2p_{3/2}$ features were consistent with the S(VI) oxidation state and assigned to the sulfate species.[17−19] In addition, the surface sulfur weight percentages presented in Table 2 were much lower than the total sulfur contents from the corresponding samples (Table 1), suggesting that sulfur preferentially diffuses from the surface to a bulk phase during the poisoning process. In view of the formation of Ce sulfates, the distribution of sulfur is related to the distribution of Ce. Furthermore, the atomic ratio of Ce/Ti (0.074) on the surface of Ce/TiO_2 is lower than the

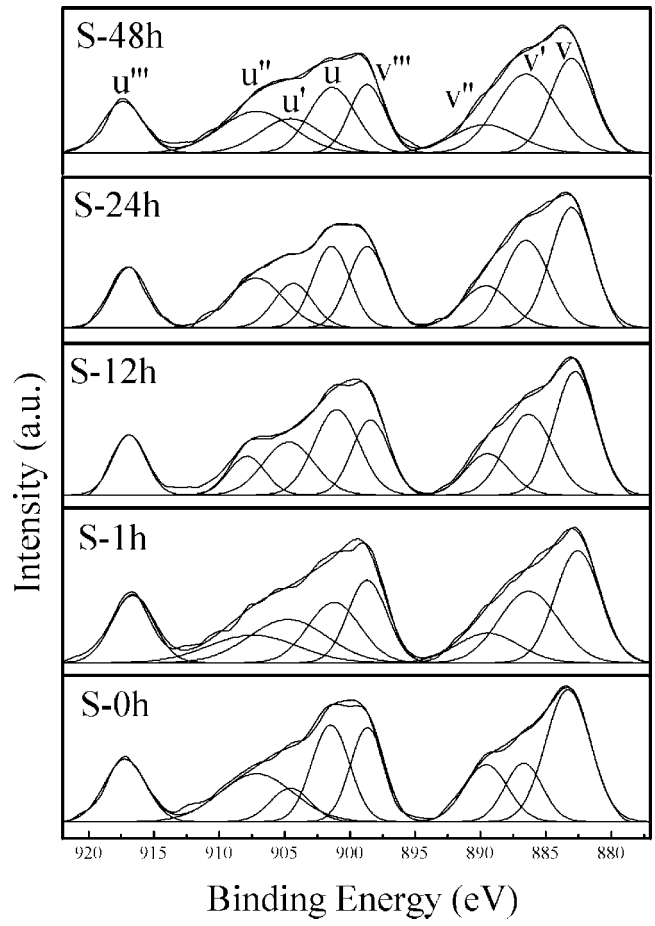

Figure 4. Experimental and fitted Ce3d XPS spectra of fresh and poisoned Ce/TiO_2 catalysts.

TABLE 2: Binding Energies of Core Electrons and Surface Weight Concentrations on the Samples

	binding energy (eV)			
sample (Ce/TiO_2)	$Ce3d_{5/2}$ (v′)	$S2p_{3/2}$	Ce(III)/Ce (%)[a]	S (%)[b]
S-0 h	886.7		22.8	
S-1 h	886.4	168.7	29.5	1.77
S-12 h	886.3	169.0	28.2	2.41
S-24 h	886.6	168.8	29.1	2.18
S-48 h	886.6	168.9	35.8	2.21

[a] Ce(III)/Ce ratio corresponds to the ratio of the peak area of the v' component relative to the total of the peak areas of all v components. [b] Weight ratio of sulfur on the surface of samples.

calculated value (0.11). Therefore, sulfur preferentially diffused from the surface to a bulk phase because of the limited exposed Ce sites.

By use of a previously described fitting procedure,[20] complex spectra in the Ce3d region were resolved into eight components. As shown in Figure 4, the peaks labeled u are due to $3d_{3/2}$ spin−orbit states, and those labeled v are the corresponding $3d_{5/2}$ states. The u'/v' doublet is attributed to the primary photoemission from Ce(III). The Ce(III)/Ce ratios in Table 2 indicate that a portion of the Ce(IV) ions transformed into Ce(III) ions as a result of Ce/TiO_2 exposure to SO_2, according to the following reaction:[20] $2CeO_2 + 3SO_2 + O_2 \rightarrow Ce_2(SO_4)_3$.

The O1s and Ti2p XPS spectra were also recorded (data not shown here). The O1s spectra exhibit that both chemisorbed oxygen and lattice oxygen species existed on the catalyst surface.[21] The Ti2p spectra show that titanium was mostly confined to its highest oxidation state (IV).[22,23] No obvious

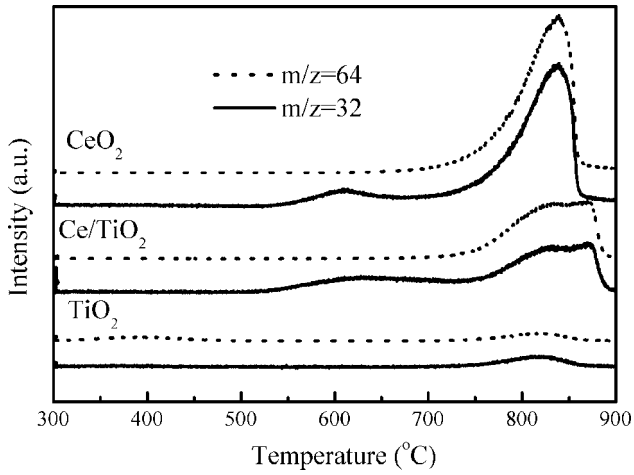

Figure 5. $SO_2 + O_2$ TPD spectra obtained at 64 and 32 amu after Ce/TiO_2, TiO_2, and CeO_2 samples were exposed to 4000 ppm SO_2 + 5% O_2 in He for 1 h at 300 °C.

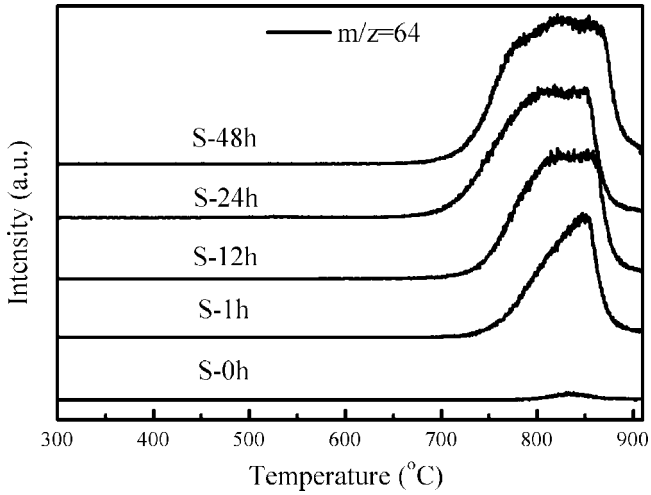

Figure 6. SO_2 TPD profiles of fresh and poisoned Ce/TiO_2 catalysts.

difference was observed from the O1s and Ti2p XPS spectra for fresh and poisoned samples.

TPD Analysis. To better understand the nature of the sulfate species formed on the poisoned samples, we examined TPD curves for Ce/TiO_2 after exposure to 4000 ppm SO_2 + 5% O_2 in He for 1 h at 300 °C. The SO_2 (m/z = 64) and the O_2 (m/z = 32) signals were monitored. For comparison, the TPD patterns of TiO_2 and CeO_2 exposed to the same conditions were also recorded. Figure 5 clearly shows two small peaks that appeared at 380 and 813 °C for TiO_2. Since no O_2 desorption occurred simultaneously with SO_2 desorption below 450 °C, the low temperature peak was assigned to the desorption of molecular SO_2.[24] The high temperature peak originated from the impurity as demonstrated by the Ce/TiO_2 TPD result (Figure 6) without any pretreatment. In contrast, a large amount of SO_2 desorbed from the surface of CeO_2 in the temperature range of 700−875 °C. These results indicate SO_2 accumulates more on CeO_2 than on TiO_2. For Ce/TiO_2, two overlapping SO_2 desorption features were observed between 750 and 900 °C. The simultaneous desorption of O_2 with SO_2 suggests that these species were associated with sulfate decomposition. On the basis of previous studies,[19,25] we suggest that the low-temperature peak is associated with the decomposition of $Ce(SO_4)_2$ and that the high-temperature peak is caused by the decomposition of $Ce_2(SO_4)_3$. Therefore, the only desorption peak due to SO_2 observed on

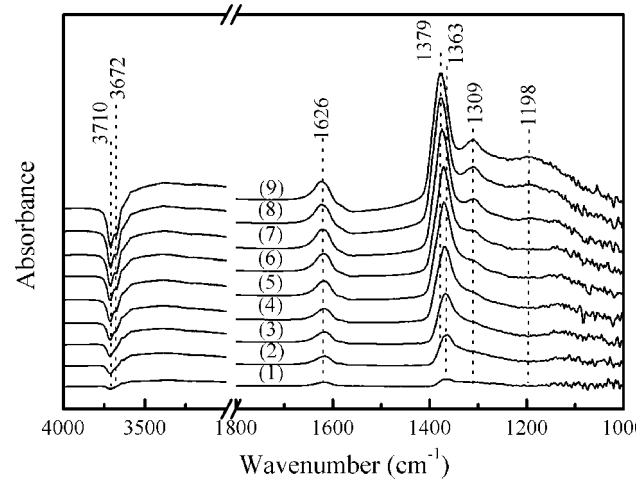

Figure 7. Changes of DRIFTS spectra of Ce/TiO_2 with time in a flow of $SO_2 + O_2$ at 300 °C (1−9) for 1, 3, 5, 10, 20, 30, 60, 120, and 180 min. (Reaction conditions: SO_2 180 ppm, O_2 5%, N_2 as balance.)

CeO_2 is assigned to $Ce(SO_4)_2$ because Ce is in an oxidation state IV. In addition, the O_2 desorption on the CeO_2 and Ce/TiO_2 samples occurred before the onset of sulfate decomposition, which was due to the composition of bulk CeO_2.

We also examined TPD experiments for fresh and poisoned Ce/TiO_2 samples by monitoring SO_2 (m/z = 64) signal, as shown in Figure 6. For the S-1 h sample, most of the SO_2 was originated from the decomposition of $Ce_2(SO_4)_3$. As poisoning time increased, the signal ascribed to the decomposition of $Ce(SO_4)_2$ emerged and increased. These results demonstrate that $Ce_2(SO_4)_3$ was more easily formed than $Ce(SO_4)_2$ during the reaction of Ce/TiO_2 with SO_2 in the presence of O_2. The present TPD results corroborate the XPS result and further support the idea that the sulfate species were formed on the catalyst, accompanied by the reduction of Ce(IV) to Ce(III). As discussed above, Ce is "locked" during the formation of high thermally stable sulfate and the redox cycle between Ce(IV) and Ce(III) is disrupted during the exposure to SO_2.

DRIFT Studies. As mentioned above, the chemical transformation of the active sites must be one of the reasons for the activity loss in the presence of SO_2. To investigate the interaction between SO_2 and the reactants over the Ce/TiO_2 catalyst, we also conducted experiments using in situ DRIFTS. First, we investigated the interaction between $SO_2 + O_2$ and the catalyst to analyze the nature of the sulfate species on the Ce/TiO_2 catalyst. Figure 7 shows the DRIFTS spectra of Ce/TiO_2 as a function of exposure time in a flow of $SO_2 + O_2$ at 300 °C. After $SO_2 + O_2$ exposure, four peaks at 1626, 1363, 1309, and 1198 cm^{-1} grew in intensity with time. According to other studies,[26,27] the peaks at 1363 and 1309 cm^{-1} can be attributed to the surface sulfate species linked to different sites, such as Ce−Ce or Ce−Ti, whereas the band at 1198 cm^{-1} can be attributed to the bulk sulfate species. The surface sulfate species band also underwent a blue shift (from 1363 to 1379 cm^{-1}) with increasing coverage of the sulfate species on Ce/TiO_2.[28] It should be noted that there was a drastic increase in the intensity of negative peaks at 3710 and 3672 cm^{-1}, which were associated with the vibration of hydroxyl groups.[29] The consumption of surface OH species means that SO_2 was able to react with surface hydroxyl groups to form adsorbed H_2O.[30,31] The synchronous growth of the band at 1626 cm^{-1} and a broadband in the range of 3300∼3500 cm^{-1} in the spectra indicate that surface water was generated. Therefore, the band at 1626 cm^{-1} is assigned to δ_{HOH} of H_2O.

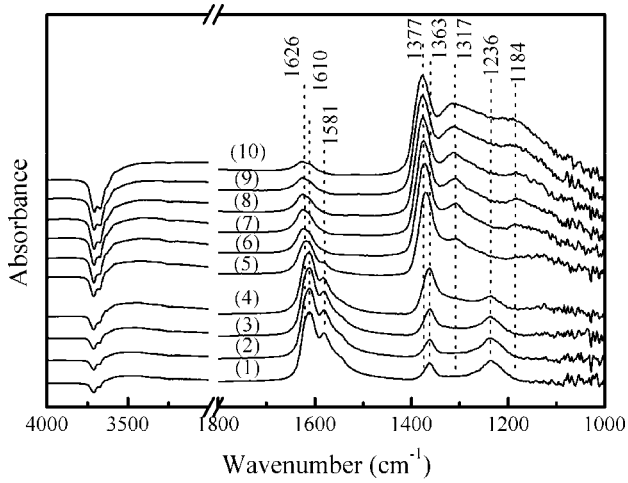

Figure 8. DRIFTS spectra of Ce/TiO_2 in a flow of NO + O_2 before and after adding 180 ppm SO_2 at 300 °C. (1) Without SO_2 for 60 min. (2−10) Adding SO_2 for 1, 3, 5, 10, 20, 30, 60, 120, and 180 min. (Reaction conditions: NO 500 ppm, O_2 5%, N_2 as balance.)

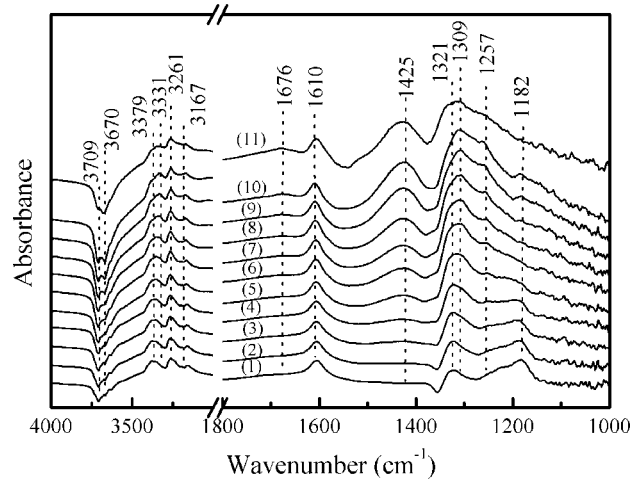

Figure 9. DRIFTS spectra of Ce/TiO_2 in a flow of NH_3 + O_2 before and after adding 180 ppm SO_2 at 300 °C. (1) Without SO_2 for 60 min. (2−10) Adding SO_2 for 1, 3, 5, 10, 20, 30, 60, 120, and 180 min. (Reaction conditions: NH_3 500 ppm, O_2 5%, N_2 as balance.) (11) DRIFTS spectrum of NH_4HSO_4-deposited Ce/TiO_2 in a flow of N_2 at 300 °C.

In principle, NO can be adsorbed in a molecular form and oxidized on oxide surfaces, giving rise to surface species such as NO^+, NO_2^-, NO_2, and NO_3^-, which were identified as key intermediates involved in SCR reactions.[32−34] Therefore, we investigated the effect of SO_2 on the oxidation of NO on the catalyst, and the results are shown in Figure 8. The bottom spectrum was obtained under a SO_2-free flow, while the other spectra were obtained in the presence of 180 ppm SO_2 with different exposure times. After exposing Ce/TiO_2 to NO + O_2 for 60 min at 300 °C, four bands at 1610, 1581, 1363, and 1236 cm^{-1} appeared, which were all due to the adsorbed nitrate species.[35,36] The addition of 180 ppm SO_2 in the feed for 10 min resulted in the appearance of a new surface sulfate species band at 1364 cm^{-1}. This band shifted to 1377 cm^{-1}, and its intensity increased sharply with exposure time. The sulfate species bands at 1317 and 1184 cm^{-1}, together with the H_2O band at 1626 cm^{-1}, also appeared upon the introduction of SO_2 and increased with time. In contrast, obvious decreases were observed for the bands of the nitrate species. These results indicate that SO_2 has a significant inhibiting effect on the formation of nitrate.

Figure 9 shows the effect of SO_2 on the oxidation of NH_3. The bottom spectrum was obtained under a SO_2-free flow. The exposure of the catalyst to a flow of NH_3 + O_2 at 300 °C for 60 min resulted in several bands. According to previous studies,[37,38] the bands at 1610 and 1182 cm^{-1} could be attributed to the asymmetric and symmetric deformation modes of coordinated NH_3 on Lewis acid sites, respectively. Bands were also found at 3379, 3331, 3261, and 3167 cm^{-1} in the NH stretching region. The band at 1321 cm^{-1} could be due to the wagging mode of an amide species (NH_2). Two negative bands at 3709 and 3670 cm^{-1} were also found, which could be from the surface hydroxyl group. The introduction of 180 ppm SO_2 into the feed resulted in the appearance of several new bands at 1676, 1425, 1309, and 1257 cm^{-1}. Their intensities increased with exposure time. The bands at 1676 and 1425 cm^{-1} were likely due to the asymmetric and symmetric deformation modes of NH_3 coordinated on Brønsted acid sites (NH_4^+).[37,38] Previous studies found that NH_4HSO_4 was stable at 300 °C and started to decompose at about 390 °C,[36] compared to ammonium sulfate ($(NH_4)_2SO_4$), which decomposed at 280 °C.[14,39−42] We deduce that NH_4HSO_4 deposited on the surface of the catalyst during the reaction between NH_3 and SO_2 in the presence of O_2. Therefore, the bands at 1676 and 1425 cm^{-1} for NH_4^+ species originated from NH_4HSO_4, and their intensities increased with the accumulation of NH_4HSO_4. Moreover, the bands at 1309 and 1257 cm^{-1}, which differed greatly from the bands at 1363 and 1309 cm^{-1} for the sulfate species in Figure 7, were supposed to be associated with HSO_4^- species that originated from NH_4HSO_4. To further examine the attribution of these bands, we examined the DRIFTS spectrum (the top spectrum in Figure 9) of the NH_4HSO_4-deposited catalyst exposed to N_2 at 300 °C, which was prepared by an impregnation method using a Ce/TiO_2 catalyst and an aqueous solution of NH_4HSO_4. As shown in Figure 9, the bands observed from the NH_4HSO_4-deposited catalyst were consistent with the results for the Ce/TiO_2 catalyst in a flow of NH_3 + O_2 after the addition of SO_2 for 180 min. It is demonstrated that NH_4HSO_4 was formed on the surface of the Ce/TiO_2 catalyst by the reaction of SO_2 and NH_3 in the presence of O_2.

To understand the deactivation mechanism of Ce/TiO_2 by SO_2 for the SCR of NO with NH_3, the DRIFTS spectra of Ce/TiO_2 in a flow of NO + NH_3 + O_2 with and without SO_2 at 300 °C were recorded and are depicted in Figure 10. The reaction was initially carried out in a steady state flow of NO + NH_3 + O_2 maintained for 60 min followed by introduction of 180 ppm SO_2 into the feed. The bottom spectrum was obtained under a SO_2-free flow, and the other spectra were obtained in the presence of 180 ppm SO_2 with different reaction times. Similarly, bands characteristic of the nitrate species (1606, 1579, and 1248 cm^{-1}), NH, NH_2, and NH_3 stretching related to NH_3 species (3150−3400, 1327, 1606, 1192 cm^{-1}) appeared in a flow of NO + NH_3 + O_2 for 60 min. Several new bands appeared at 1680, 1427, 1309, and 1257 cm^{-1} upon introduction of SO_2. The bands at 1309 and 1257 cm^{-1} associated with HSO_4^- species were unclear because they overlapped adjacent peaks at 1327 (NH_2 species) and 1248 cm^{-1} (nitrate species), respectively. Moreover, their intensities increased gradually with time. As a result, a combined band centered at 1277 cm^{-1} was observed in Figure 10. The intensities of the bands at 1680 and 1427 cm^{-1} due to NH_4^+ species also increased with time, which is consistent with the phenomena presented in Figure 9. In contrast, the bands for nitrate species promptly decreased with increasing SO_2 exposure time, while the bands attributed to NH

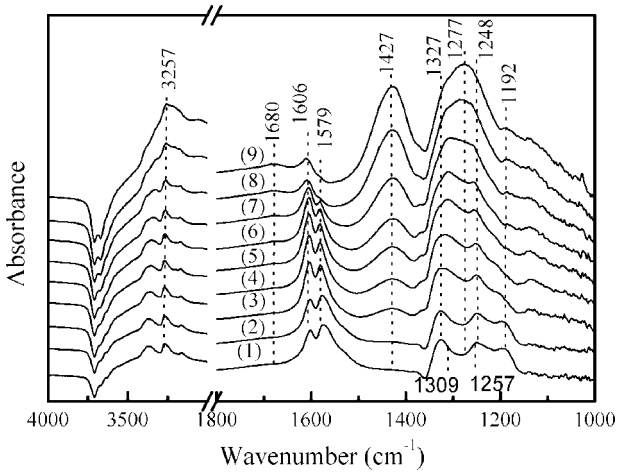

Figure 10. DRIFTS spectra of Ce/TiO_2 in a flow of NO + NH_3 + O_2 before and after adding 180 ppm SO_2 at 300 °C. (1) Without SO_2 for 60 min. (2−9) Adding SO_2 for 1, 5, 10, 20, 30, 60, 120, and 180 min. (Reaction conditions: NO 500 ppm, NH_3 500 ppm, O_2 5%, N_2 as balance.)

and NH_3 species remained almost unchanged. These results suggest that the addition of SO_2 not only inhibits the formation of nitrate but also results in the formation of NH_4HSO_4 in the SCR reaction, which could deposit on the surface of the catalyst and block the active sites.

We observed that the effect of deposited NH_4HSO_4 was crucial for the deactivation of the catalyst based on our DRIFTS results. However, there were no SO_2 desorption peaks starting around 390 °C in Figure 6, which could be ascribed to the decomposition of NH_4HSO_4. This may be associated with the different sensitivities of mass spectrometry (MS) and DRIFTS. DRIFTS is a surface-sensitive technology and only provides insight into the formation of surface NH_4HSO_4, while the species formed in the bulk phase cannot be detected. On the other hand, ammonia, which is one of the decomposition products of NH_4HSO_4, was undistinguishable from H_2O by MS because they exhibited the same signal of $m/z = 17$. The other sulfate products may have been left on the surface of the samples and combined with Ce to form more stable $Ce(SO_4)_2$ and $Ce_2(SO_4)_3$. In that case, we would only have observed SO_2 as a decomposition product of Ce sulfate.

Combined with the activity results of the Ce/TiO_2 catalyst in Figure 1, we estimated that the decrease in NO conversion in the presence of SO_2 during the first 12 h was caused by the deposition of NH_4HSO_4 on the surface of the Ce/TiO_2 catalyst, which could block the active sites of the catalyst and reduce its specific area. However, our results suggest that the formation of NH_4HSO_4 is not the main deactivation route because of the limited sulfur coverage on the surface of the catalyst. The further decrease in NO conversion in the following 36 h was a result of a change in the catalyst. We theorize that the formation of $Ce(SO_4)_2$ and $Ce_2(SO_4)_3$ is the primary reason for the permanent deactivation of the Ce/TiO_2 catalyst due to their high thermal stability. The formation of $Ce(SO_4)_2$ and $Ce_2(SO_4)_3$ disrupts the redox process between Ce(IV) and Ce(III), which is crucial for the adsorption and activation of reactants during the SCR reaction. Another factor affecting the deactivation is the inhibiting effect of sulfate on the formation and adsorption of the nitrate species, which is known to be one of the key intermediates during the SCR reaction, especially at low temperatures.

Furthermore, when the reaction temperature increased from 300 to 350 °C and the concentration level of SO_2 remained the same, the negative effects from SO_2 were noticeably weaker. This suggests that at low temperatures, the SCR reaction over the Ce/TiO_2 catalyst may occur via the Langmuir−Hinshelwood mechanism since the activity decreased when the adsorption of nitrate was inhibited by the formative sulfate species. On the other hand, the SCR reaction may follow the Eley−Rideal mechanism at high temperatures because of the small association between the adsorbed nitrate species and the reaction activity. More detailed investigation of the SCR reaction mechanism over the Ce/TiO_2 catalyst will be conducted.

Conclusions

The presence of SO_2 in the feed gas led to a permanent deactivation of the SCR of NO by NH_3 over the Ce/TiO_2 catalyst. The lower the reaction temperature the greater the negative effect of SO_2 was. In the presence of O_2, NH_3 can easily react with SO_2 to favor the formation of NH_4HSO_4, which can deposit on the surface of the catalyst and block the active sites. The formative $Ce(SO_4)_2$ and $Ce_2(SO_4)_3$ on Ce/TiO_2 have high thermal stability and not only inhibit the formation of nitrate but also "lock" the cerium cation and disrupt the Ce(IV)/Ce(III) redox cycle. Both of these mechanisms are necessary for the SCR reaction. This is shown to be the primary reason for the deactivation of the Ce/TiO_2 catalyst during the SCR of NO by NH_3 in the presence of SO_2. Therefore, we conclude that the Ce/TiO_2 catalyst is only suitable for practical applications in sulfur-free or low-sulfur gas streams. The addition of other promoters to inhibit the oxidation of SO_2 to form sulfate should be considered for further improvement of sulfur tolerance using this type of catalyst.

Acknowledgment. This work was financially supported by the Ministry of Science and Technology of China (2004CB719503, 2006AA060304) and the National Natural Science Foundation of China (20425722).

References and Notes

(1) Bosch, H.; Janssen, F. *Catal. Today* **1988**, *2*, 369.
(2) Forzatti, P. *Catal. Today* **2000**, *62*, 51.
(3) Müller, W.; Ölschlegel, H.; Schäfer, A.; Hakim, N.; Binder, K. SAE, 2003, 2003−01−2304.
(4) Busca, G.; Lietti, L.; Ramis, G.; Berti, F. *Appl. Catal., B* **1998**, *18*, 1.
(5) Lietti, L.; Nova, I.; Ramis, G.; Dall'Acqua, L.; Busca, G.; Giamello, E.; Forzatti, P.; Bregani, F. *J. Catal.* **1999**, *187*, 419.
(6) Ma, A. Z.; Grünert, W. *Chem. Commun.* **1999**, 71.
(7) Carja, G.; Delahay, G.; Signorile, C.; Coq, B. *Chem. Commun.* **2004**, 1203.
(8) Tang, X.; Hao, J.; Xu, W.; Li, J. *Catal. Commun.* **2007**, *8*, 329.
(9) Ramis, G.; Yi, L.; Busca, G.; Turco, M.; Kotur, E.; Willey, R. J. *J. Catal.* **1995**, *157*, 523.
(10) Liu, F.; He, H.; Zhang, C. *Chem. Commun.* **2008**, 2043.
(11) Xu, W.; Yu, Y.; Zhang, C.; He, H. *Catal. Commun.* **2008**, *9*, 1453.
(12) Kijlstra, W. S.; Biervliet, M.; Poels, E. K.; Bliek, A. *Appl. Catal., B* **1998**, *16*, 327.
(13) Nam, I.-S.; Eldridge, J. W.; Kittrell, J. R. *Ind. Eng. Chem. Prod. Res. Dev.* **1986**, *25*, 192.
(14) Choo, S. T.; Yim, S. D.; Nam, I.-S.; Ham, S.-W.; Lee, J.-B. *Appl. Catal., B* **2003**, *44*, 237.
(15) Nakajima, F.; Hamada, I. *Catal. Today* **1996**, *29*, 109.
(16) Ferrizz, R. M.; Gorte, R. J.; Vohs, J. M. *Catal. Lett.* **2002**, *82*, 123.
(17) Smirnov, M. Y.; Kalinkin, A. V.; Pashis, A. V.; Sorokin, A. M.; Noskov, A. S.; Kharas, K. C.; Bukhtiyarov, V. I. *J. Phys. Chem. B* **2005**, *109*, 11712.
(18) Rodriguez, J. A.; Jirsak, T.; Freitag, A.; Hanson, J. C.; Larese, J. Z.; Chaturvedi, S. *Catal. Lett.* **1999**, *62*, 113.
(19) Xie, G.; Liu, Z.; Zhu, Z.; Liu, Q.; Ge, J.; Huang, Z. *J. Catal.* **2004**, *224*, 42.
(20) Damyanova, S.; Perez, C. A.; Schmal, M.; Bueno, J. M. C. *Appl. Catal., A* **2002**, *234*, 271.

(21) Yang, S.; Feng, Y.; Wan, J.; Zhu, W.; Jiang, Z. *Appl. Surf. Sci.* **2005**, *246*, 222.
(22) Reddy, B. M.; Khan, A.; Yamada, Y.; Kobayashi, T.; Loridant, S.; Volta, J.-C. *J. Phys. Chem. B* **2003**, *107*, 5162.
(23) González, I. D.; Navarro, R. M.; Álvarez-Galván, M. C.; Rosa, F.; Fierro, J. L. G. *Catal. Commun.* **2008**, *9*, 1759.
(24) Chen, Y.; Jiang, Y.; Li, W.; Jin, R.; Tang, S.; Hu, W. *Catal. Today* **1999**, *50*, 39.
(25) Luo, T.; Vohs, J. M.; Gorte, R. J. *J. Catal.* **2002**, *210*, 397.
(26) Luo, T.; Gorte, R. J. *Appl. Catal., B* **2004**, *53*, 77.
(27) Waqif, M.; Bazin, P.; Saur, O.; Lavalley, J. C.; Blanchard, G.; Touret, O. *Appl. Catal., B* **1997**, *11*, 193.
(28) Wu, Q.; Gao, H.; He, H. *J. Phys. Chem. B* **2006**, *110*, 8320.
(29) Yates, D. J. C. *J. Phys. Chem.* **1961**, *65*, 746.
(30) Goodman, A. L.; Bernard, E. T.; Grassian, V. H. *J. Phys. Chem. A* **2001**, *105*, 6443.
(31) Ma, Q.; Liu, Y.; He, H. *J. Phys. Chem. A* **2008**, *112*, 6630.
(32) Ito, E.; Hultermans, R. J.; Lugt, P. M.; Burgers, M. H. W.; Rigutto, M. S.; van Bekkum, H.; van den Bleek, C. M. *Appl. Catal., B* **1994**, *4*, 95.
(33) Kapteijn, F.; Singoredjo, L.; Dekker, N. J. J.; Moulijn, J. A. *Ind. Eng. Chem. Res.* **1993**, *32*, 445.
(34) Centi, G.; Perathoner, S. *Appl. Catal., A* **1995**, *132*, 179.
(35) Underwood, G. M.; Miller, T. M.; Grassian, V. H. *J. Phys. Chem. A* **1999**, *103*, 6184.
(36) Kantcheva, M. *J. Catal.* **2001**, *204*, 479.
(37) Ito, E.; Mergler, Y. J.; Nieuwenhuys, B. E.; Calis, H. P. A.; van Bekkum, H.; van den Bleek, C. M. *J. Chem. Soc., Faraday Trans.* **1996**, *92*, 1799.
(38) Qi, G.; Yang, R. T. *J. Phys. Chem. B* **2004**, *108*, 15738.
(39) Hirota, K.; Mäkelä, J.; Tokunaga, O. *Ind. Eng. Chem. Res.* **1996**, *35*, 3362.
(40) Notoya, F.; Su, C.; Sasaoka, E.; Nojima, S. *Ind. Eng. Chem. Res.* **2001**, *40*, 3732.
(41) Phil, H. H.; Reddy, M. P.; Kumar, P. A.; Ju, L. K.; Hyo, J. S. *Appl. Catal., B* **2008**, *78*, 301.
(42) Zhu, Z.; Niu, H.; Liu, Z.; Liu, S. *J. Catal.* **2000**, *195*, 268.

JP8088148